Materials Research Bulletin 46 (2011) 748–754

Contents lists available at ScienceDirect

Materials Research Bulletin

journal homepage: www.elsevier.com/locate/matresbu

Facile preparation of carbon coated magnetic Fe_3O_4 particles by a combined reduction/CVD process

Juliana C. Tristão [a], Aline A.S. Oliveira [a], José D. Ardisson [b], Anderson Dias [c], Rochel M. Lago [a,*]

[a] Departamento de Química, Universidade Federal de Minas Gerais, Belo Horizonte-MG, 31270-901, Brazil
[b] Laboratório de Física Aplicada, CDTN, Belo Horizonte, MG 30123-970, Brazil
[c] Departamento de Química, Universidade Federal de Ouro Preto, Ouro Preto-MG, 35400-000, Brazil

ARTICLE INFO

Article history:
Received 20 June 2010
Received in revised form 1 December 2010
Accepted 12 January 2011
Available online 19 January 2011

Keywords:
A. magnetic materials
B. vapor deposition
D. surface properties

ABSTRACT

In this work, we report a simple method for the preparation of magnetic carbon coated Fe_3O_4 particles by a single step combined reduction of Fe_2O_3 together with a Chemical Vapor Deposition process using methane. The temperature programmed reaction monitored by Mössbauer, X-ray Diffraction and Raman analyses showed that Fe_2O_3 is directly reduced by methane at temperatures between 600 and 900 °C to produce mainly Fe_3O_4 particles coated with up to 4 wt% of amorphous carbon. These magnetic materials can be separated into two fractions by simple dispersion in water, i.e., a settled material composed of large magnetic particles and a suspended material composed of nanoparticles with an average size of 100–200 nm as revealed by Scanning Electron Microscopy and High-resolution Transmission Electron Microscopy. Different uses for these materials, e.g., adsorbents, catalyst supports, rapid coagulation systems, are proposed.

1. Introduction

Magnetic particles have many potential technological applications in different areas, e.g., in catalysis as support [8,9], in biomedicine as magnetic resonance imaging [5,6] and in drug delivery [7], in adsorption processes [10] and in environmental remediation [1–4]. Magnetic particles can be coated with a protective layer of different materials to improve their stability and to introduce new surface properties and functionalities. Some of these coating materials are silica [11], alumina [12], gold [13], and polymers, such as polystyrene [14], polyaniline [15], polymethyl methacrylate [16] and polyacrylamide [17]. Carbon is a versatile coating material due to its chemical stability, biocompatibility, possibility of surface modification and pore creation. Carbon coated Fe^o or carbide particles can be produced by different methods, such as arch discharge (e.g., Fe [18], SiO_2/Fe [19], Al_2O_3/Fe [20]), plasma discharge (e.g., Fe_3C [21]), pyrolysis of metallic complexes (e.g., CNT/FeRu [22]), explosive reaction (e.g., Fe_7C_3 [23]). and chemical vapor deposition (CVD), i.e., C/Fe [24], CNT/Fe [25], C/Ni [26], C/Fe_3C/Fe_2O_3 [27]. On the other hand, carbon coated magnetite is more difficult to obtain due to the facile reduction of Fe_3O_4 to Fe^o and carbide under typical reaction conditions. The few works described in the literature are based on the precipitation of Fe oxide nanoparticles followed by stabilization with tensioactive molecules (oleic acid or CTBA). The stabilized nanoparticles are then mixed with different organic carbon precursors, e.g., glucose, PEG, citric acid, and treated hydrothermically at temperatures of 200–600 °C [28–33].

In general, these carbon coating processes are relatively complex, demanding special precursors and producing relatively low yields [10,34]. In this work, we report for the first time a simple procedure to prepare magnetic particles based on Fe_3O_4 cores coated by carbon via a simultaneous iron reduction/carbon deposition process. In this process, methane reduces Fe_2O_3 with very good selectivity to Fe_3O_4 magnetic nuclei and leads to carbon deposition by a CVD reaction (Fig. 1).

This technically simple method can use as precursor different iron containing materials, such as synthetic (Fe_2O_3, Fe_3O_4, FeOOH, etc.) and naturally occurring iron oxides or even iron containing wastes (e.g., red mud, and mining waste). We also present a preliminary work on the use of these magnetic particles as adsorbent and for the production of a magnetic recyclable supported Pd catalyst.

2. Experimental

The hematite was prepared by heating 5 g of hydrated ferric nitrate ($Fe(NO_3)_3{\cdot}9H_2O$) in air at 5 °C min^{-1} up to 400 °C during 3 h.

* Corresponding author at: Universidade Federal de Minas Gerais, Departamento de Química, Av. Antonio Carlos, 6627, 31270-901 Belo Horizonte, Minas Gerais, Brazil. Tel.: +55 31 34095719; fax: +55 31 3409 5700.
E-mail address: rochel@ufmg.br (R.M. Lago).

0025-5408/$ – see front matter © 2011 Elsevier Ltd. All rights reserved.
doi:10.1016/j.materresbull.2011.01.008

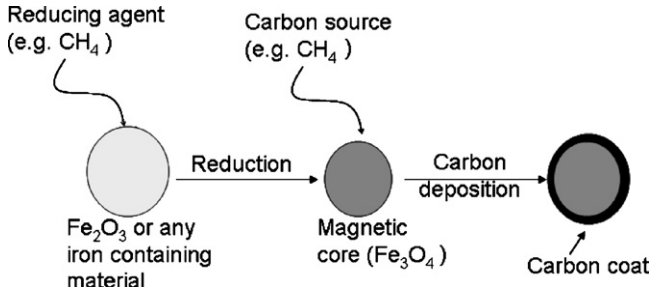

Fig. 1. Schematic representation of the reduction of Fe_2O_3 and carbon coating.

The TPRe (Temperature Programmed Reaction) studies were carried out reacting hematite (100 mg) with ca. 5% methane in N_2 (30 mL min^{-1}) and hematite (100 mg) in a quartz tube of 7 mm diameter heated at 5 °C min^{-1} up to 900 °C. The reaction was interrupted at different temperatures, i.e., 600, 700, 800, 900, 950 °C and was also maintained for 1 h and 3 h at 900 °C. The samples were named HtM followed by temperature and time of reaction, i.e., HtM600 and HtM900/1 h. The gas mixture was directly analyzed by gas chromatography (Shimadzu GC17A) with a FID (Flame Ionization Detector) using automatic injection every 3 min. The chromatographic conditions were: injector 150 °C, column (Carbowax) 60 °C, FID 200 °C and split 1:30. Fig. 2 shows the scheme of the TPRe studies.

The samples were characterized by X-ray diffraction (XRD), Mössbauer spectroscopy, magnetization measurements, thermal analysis (TG), Raman spectroscopy, BET surface area, scanning electron microscopy (SEM) and high-resolution transmission electron microscopy (HRTEM) before and after the TPRe.

The powder XRD data were obtained in a Rigaku equipment model Geigerflex using Co Kα radiation, scanning from 10 to 80° (2θ) at a scan rate of 4° min^{-1}. Silicon was used as an external standard. The crystallite sizes were determined by Scherrer's equation through the width of the Bragg reflection at half maximum. The transmission Mössbauer spectroscopic experiments were carried out in a CMTE spectrometer model MA250 with a $^{57}Co/Rh$ source at room temperature using α-Fe as a reference. The magnetization measurements were carried out in a portable magnetometer with a fixed magnetic field of 0.3 T. TG analyses were carried out in a Shimadzu TGA-60, with a constant heating rate of 10 °C min^{-1} under an air flow (100 mL min^{-1}). Raman spectroscopy by was carried out using a Horiba/Jobin-YvonLABRAM-HR spectrometer. Experimental data were obtained with the 632.8 nm line of a helium–neon laser (effective power of 6 mW at the sample's surface) as excitation source, diffraction

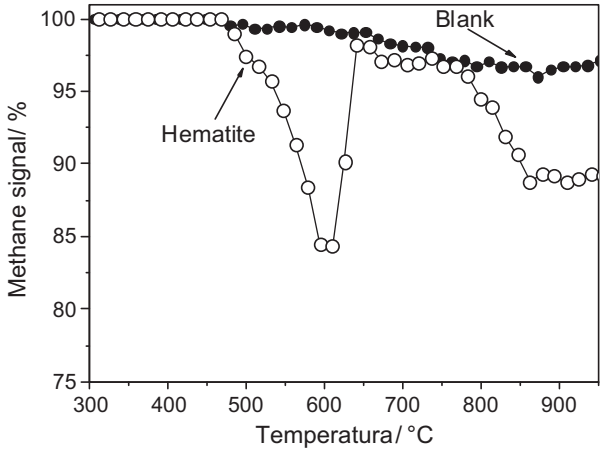

Fig. 2. TPRe profile for hematite (Fe_2O_3) reaction with methane.

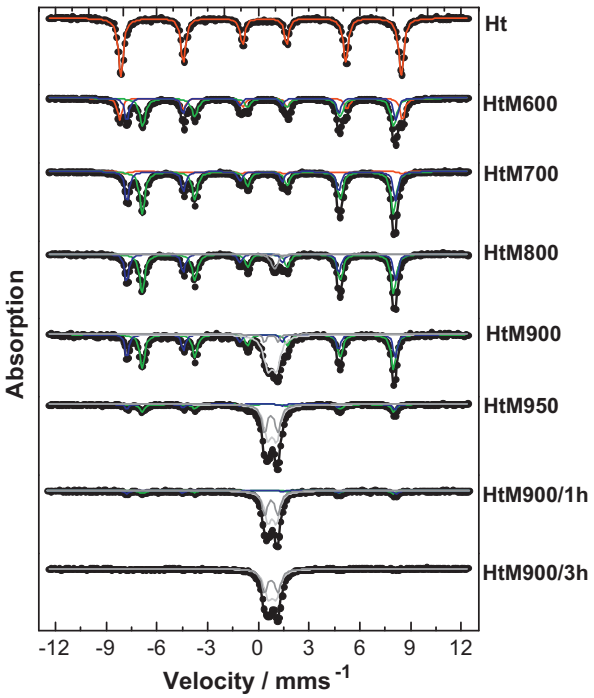

Fig. 3. Mössbauer spectra of hematite after reaction with methane interrupted at different temperatures and times: 600, 700, 800, 900, 950 °C and 900 °C, 1 h and 3 h.

gratings of 600 and 1800 grooves/mm, Peltier-cooled CCD detector, confocal Olympus microscope (100 × objective), and experimental resolution of typically 1 cm^{-1} for 10 accumulations of 30 s. The surface area was determined by nitrogen adsorption using the BET method with a 22 cycles N_2 adsorption/desorption in an Autosorb 1 Quantachrome instrument. Scanning electron microscopy (SEM) analysis was done using Jeol JSM 840A and Quanta 200 ESEM FEG equipments. Transmission electron microscopy (TEM) analysis was done using a Tecnai G2-20 obtained from FEI.

Batch equilibrium experiments were used in the adsorption tests employing 10 mg of the material and 10 mL of 50 mgL^{-1} of chlorobenzene. All solutions were kept for 24 h at room temperature. The concentration of chlorobenzene was measured by UV/vis spectrophotometry using an UVmini-1240 equipment.

The hydro-dechlorination of chlorobenzene to benzene was studied using a Pd catalyst supported on the materials. The catalyst Pd(5%)/HtM700 was prepared by impregnation of palladium acetate on the sample HtM700 (after reaction with methane at 700 °C) and subsequent reduction. The catalytic tests were carried out with 50 mg of Pd(5%)/HtM700 in 20 mL of ethanol containing 0.5% m/v of chlorobenzene and 0.5% m/v of toluene (internal standard). The acid produced with reaction was neutralized with 0.2 g of NaOH. Under a H_2 atmosphere, the system was immersed in an oil bath at 100 °C, while stirring. Samples were taken from the reaction at different times, i.e., 0, 15, 30, 45 and 60 min and analyzed by gas chromatography (Shimadzu GC17A) with a FID detector. For the catalyst reuse, the chlorobenzene solution was discharged after 60 min of reaction and the system was loaded with a new solution, while the catalyst was magnetically secured.

3. Results and discussion

3.1. Reaction of Fe_2O_3 with methane

The reaction of methane with synthetic hematite Fe_2O_3 was investigated using a temperature programmed reaction (TPRe) system. TPRe showed that methane reacts with hematite in the

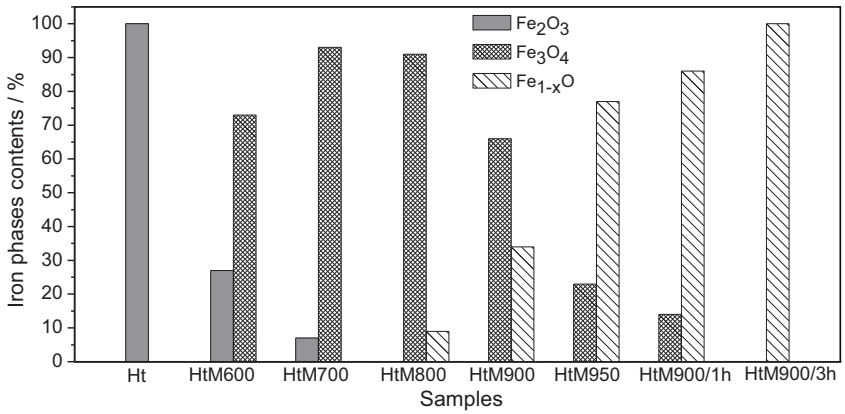

Fig. 4. Iron phases contents over the different temperatures and times of reaction of hematite and methane.

temperature ranges of 450–680 °C and of 750–900 °C (Fig. 2). Blank experiments (absence of Fe_2O_3) showed no significant thermal reaction of methane up to 900 °C.

In order to investigate the iron phases formed in each step, the TPRe experiments were interrupted at different temperatures, i.e., 600, 700, 800 and 900 °C, by quenching the reactor. The samples were named as follows HtM600 (hematite reduced with methane at 600 °C) and characterized by Mössbauer spectroscopy, XRD, magnetization measurements, BET surface area, elemental analysis, thermal analysis, Raman spectroscopy, SEM and TEM.

The Mössbauer spectra obtained after TPRe with methane are shown in Fig. 3. The hyperfine parameters are presented in the Supplementary Material. The Mössbauer spectrum of hematite before the reaction shows a sextet related to the α-Fe_2O_3 phase. After TPRe with methane at 600 °C, the relative area of the Fe_2O_3 sextet decreases (from 100 to 27%) and splits into two new sextets assigned to octahedric and tetrahedric sites of the magnetite phase, Fe_3O_4, with 47 and 26% of area, respectively. At 700 °C methane almost completely reduces Fe_2O_3 to magnetite (93% relative area). For higher temperatures, two duplets can be observed related to the presence of Fe^{3+} and Fe^{2+} from the wüstite phase. At higher temperatures and longer reaction times wüstite is the main phase formed, e.g., 100% $Fe_{1-x}O$ at 900 °C/3 h.

Fig. 4 summarizes the iron phase contents obtained by Mössbauer after reaction with methane at different temperatures. There is a gradual decrease of the hematite phase up to 700 °C. At 600 °C the magnetite phase is formed with a maximum at 700 °C and a continuous decrease until 900 °C/1 h. The wüstite phase appears at 800 °C and at 900 °C/3 h is the only phase present.

XRD analyses (Supplementary Material) completely agreed with the Mössbauer data showing that the α-Fe_2O_3 phase, with crystallite size of 22 nm, is gradually reduced to magnetite (Fe_3O_4) and wüstite ($Fe_{1-x}O$) as the reaction temperature increases. The iron phases identified show an increase of the crystallite size at high reaction temperatures, i.e., the magnetite phase varies from 34 to 49 nm whereas the wüstite phase from 25 to 46 nm. These results coupled with TCD/GC analyses indicate that methane reduces Fe_2O_3 according to the simplified reactions shown in Eqs. (1) and (2).

$$15Fe_2O_3 + CH_4 \rightarrow 10Fe_3O_4 + 2H_2O + CO \quad (1)$$

$$5Fe_3O_4 + CH_4 \rightarrow 15FeO + 2H_2O + CO \quad (2)$$

Magnetizations of 0, 62, 91, 88, 59, 14 and 3 J T^{-1} kg^{-1} were obtained for Ht and for the samples after TPRe with methane, HtM600, HtM700 HtM800 HtM900, HtM950 and HtM900/1 h, respectively (Table 1). These results show that all materials after TPRe are magnetic and that this property is dependent on the magnetite phase content. The reaction with methane also causes two other effects: (i) the reduction of the surface area and (ii) carbon deposition. The BET surface area decreases from 17 m^2 g^{-1} for pure hematite (Ht) to 0.2–6.0 m^2 g^{-1} after methane TPRe (Table 1). TPCVD (Temperature Programmed Chemical Vapor Deposition) [35] experiments (Supplementary Material) clearly showed the formation of H_2 at temperatures higher than ca. 700 °C which is related to carbon deposition according to the simplified Eq. (3)):

$$CH_4 \rightarrow C + 2H_2 \quad (3)$$

The carbon content of the obtained materials was determined by elemental analysis and from TG weight loss. The presence of ca. 2–4% of carbon was observed in most of the materials (Table 1).

Table 1
Surface area, saturation magnetization and carbon content for the samples obtained after TPRe of Fe_2O_3 with methane at different temperatures.

Sample	BET surface area/m^2 g^{-1}	Saturation magnetization/JT^{-1} kg^{-1}	C content[a]/wt%
Ht	17.0	0	0
HtM600	6.0	62	2.5[a] (0.8)[b]
HtM700	3.0	91	3.9[a] (4.4)[b]
HtM800	0.4	88	3.7[a] (2.8)[b]
HtM900	0.4	59	3.0[a] (2.6)[b]
HtM950	0.4	14	– (4.0)[b]
HtM900/1 h	0.4	3	– (3.0)[b]
HtM900/3 h	0.2	–	4.0[a]

[a] Determined by elemental analysis.
[b] Determined from TG results.

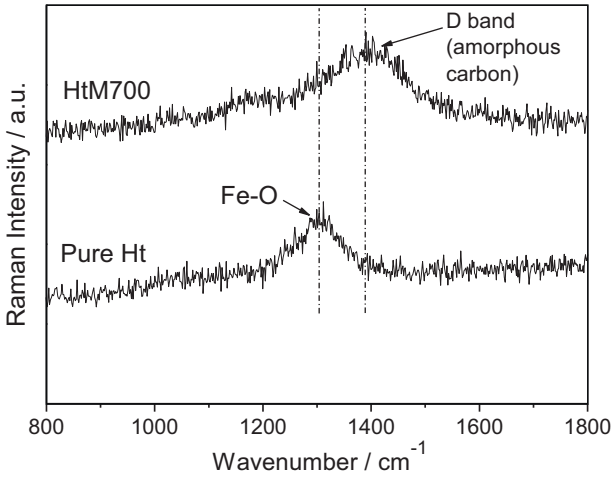

Fig. 5. Raman spectra of pure Fe_2O_3 and the sample HtM700.

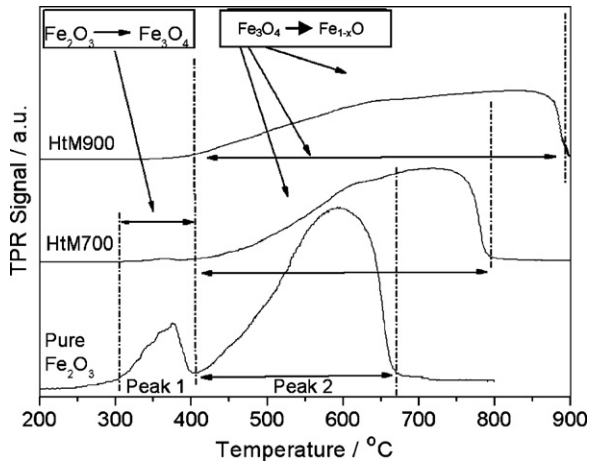

Fig. 6. Temperature programmed reduction of pure Fe_2O_3 and the samples HtM700 and 900.

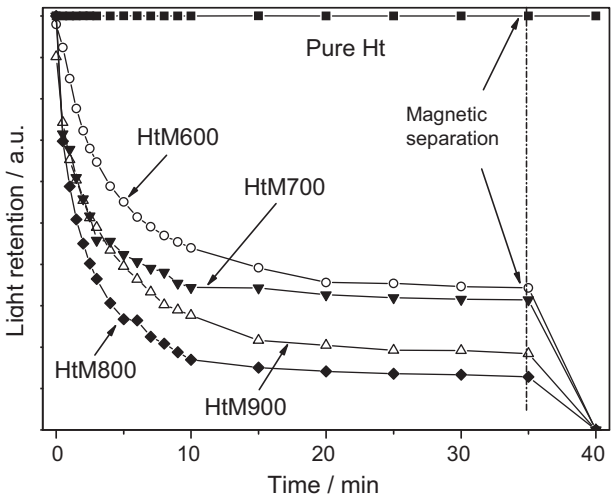

Fig. 7. Temperature programmed reduction of pure Fe_2O_3 and the samples HtM700 and 900.

Raman analysis (Fig. 5) shows that upon reaction with methane at 700 °C, the characteristic band for Fe_2O_3 centered at 1300 cm^{-1} disappears and a new band at 1380 cm^{-1} can be observed. This new band is related to the well known D band [30] due to the presence of defective carbonaceous structures, e.g., amorphous carbon. No band was observed at ca. 1600 cm^{-1} (G band), suggesting the absence of more organized carbon, such as graphite.

Pure Fe_2O_3 and the samples HtM700 and HtM900 were also submitted to a temperature programmed reduction (TPR) with H_2 (Fig. 6). Hematite shows a peak between 300 and 400 °C (Peak 1) due to the reduction to form Fe_3O_4 [4]. A second broad peak (Peak 2) between 400 and 670 °C is related to the sequential reduction of Fe_3O_4 to FeO and Fe^o [4]. After reaction with methane at 700 °C, Peak 1 cannot be observed due to the absence of the Fe_2O_3 phase consumed in the CVD process. Peak 2 appears broadened and the reduction finishes at much higher temperature, i.e., 800 °C. Similar effects are observed for the sample HtM900 with the final reduction temperature at ca. 900 °C. These results clearly indicate that the Fe_3O_4 and FeO present in the composites HtM700 and 900 are much more difficult to reduce compared to the pure oxides. This effect is likely due to an encapsulation of the iron oxides by carbon, which hinders the reduction process.

The magnetic materials produced by reaction of hematite with methane were dispersed in water by sonication for 5 min. The decantation rate of the particles was followed by simple light transmission measurements at three different wavelengths (450, 600 and 750 cm^{-1}). The obtained results are displayed in Fig. 7.

It can be observed for pure hematite before the reaction with methane that the solid particles remain in stable suspension for 40 min. On the other hand, for the sample HtM600 a rapid sedimentation is observed reaching 40% of light retention within

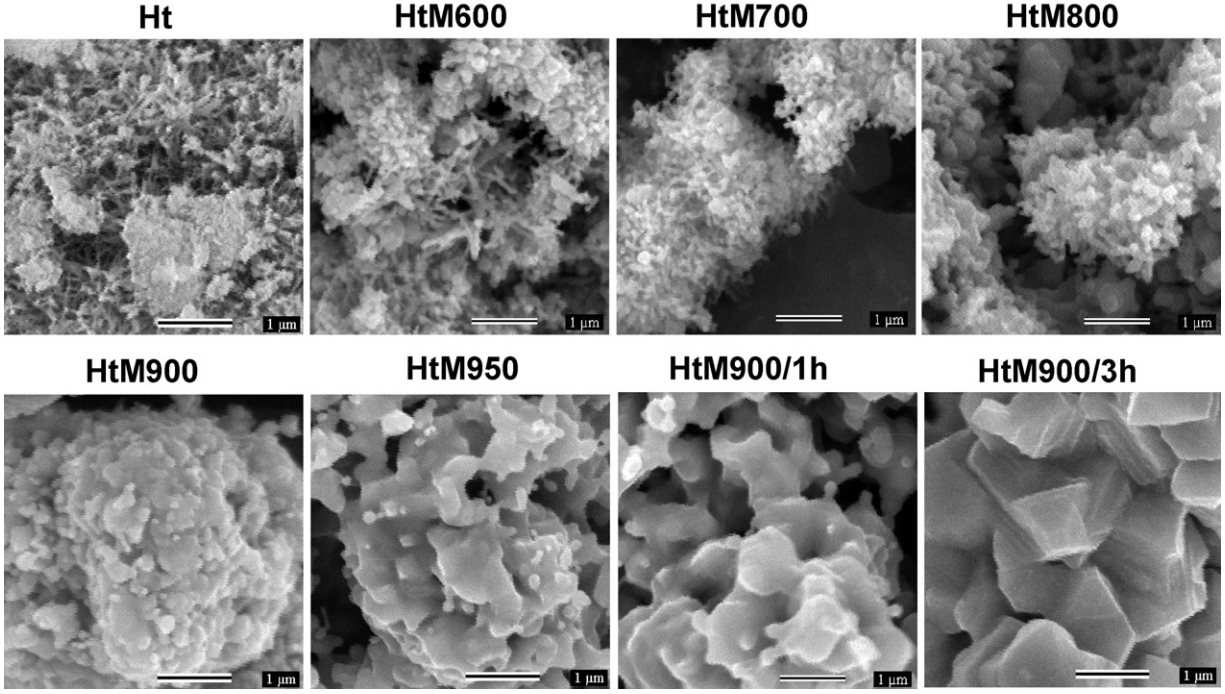

Fig. 8. SEM images of the settled particles of HtM600, 700, 800, 900, 950 °C and 900 °C, 1 h and 3 h (scale bar = 1 μm).

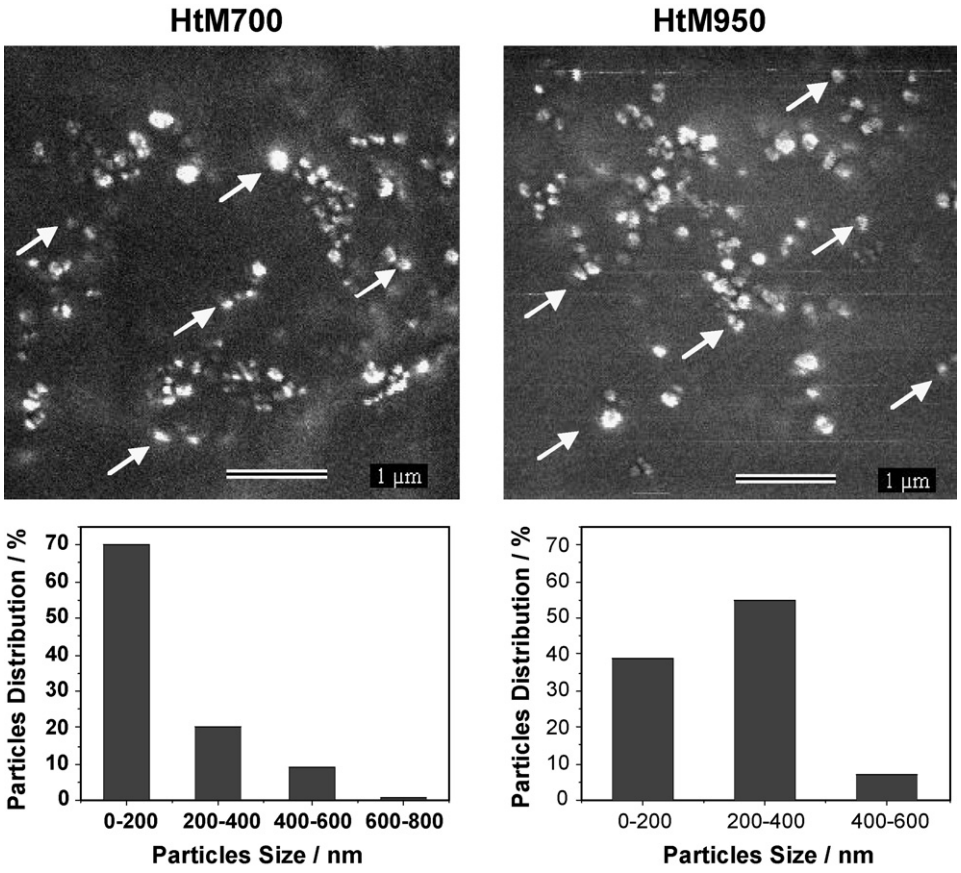

Fig. 9. SEM image and particles size estimation for the suspension of the samples HtM700 and HtM950 dispersed in water.

ca. 15 min. As the CVD temperature is increased to 700 and 800 °C, the sedimentation rate increases. After ca. 20 min all suspensions seem to be stable. The material remaining in suspension is magnetic since simple approximation of a magnet removes all the particles from the suspension (Supplementary Material). The amount of suspended material was obtained by simple separation of the settled material from the suspension after 35 min, followed by drying overnight and weighting. The HtM600, 700, 800 and 900 samples show fractions of suspended particles of ca. 5, 5, 3 and 4 wt%, respectively.

The settled materials were analyzed by SEM and the images are shown in Fig. 8.

Fig. 8 suggests that the CVD carried out up to 800 °C do not cause significant changes of the material morphology. On the other hand, at 900 and 950 °C the reaction with methane causes a strong sintering with formation of well defined particle surfaces.

After dispersion in water, the material remaining in suspension was analyzed by SEM and the particles size distribution was estimated.

Fig. 9 suggests that after reaction with methane at 700 °C (HtM700) and 950 °C (HtM950) 70 and 39% of the particles in suspension have a size smaller than 200 nm. Detailed analysis of the sample HtM700 is shown in Fig. 10.

SEM analysis of the HtM700 suspended particles (Fig. 10a) shows the presence of spherical particles with average size of 200 nm. TEM images (Fig. 10b and c) revealed fringes of 4.5 Å, which correspond to the d space of Fe_3O_4. This value is similar to the d space calculated based on DRX data (4.4 Å). TEM also showed the presence of amorphous material on the particle surface which could be related to non crystalline iron oxides and also amorphous carbon.

Preliminary adsorption studies were carried out using chlorobenzene as a hydrophobic model compound. Fig. 11 shows the obtained results.

Pure hematite (Ht) does not adsorb the hydrophobic chlorobenzene. This is related to the more hydrophilic character of the hematite surface. However, for all materials produced by reaction with methane a significant adsorption of chlorobenzene is observed. The results clearly show that carbon deposited on the magnetite surface favors the adsorption of apolar chlorobenzene.

The material HtM700 was also used in preliminary tests as magnetic support for a Pd catalyst used in hydrodechlorination of chlorobenzene (Eq. (4)).

$$C_6H_5Cl + H_2 \rightarrow C_6H_6 + HCl \quad (4)$$

The HCl produced during the hydrodechlorination reaction is very aggressive and can potentially attack and deactivate the catalyst, especially the unprotected Fe_3O_4 support.

Fig. 12 shows the TONs (turnover numbers) for the 1st use and for three consecutive reuses of the catalyst.

It can be observed that the fresh catalyst Pd (5%)/HtM700 converted about 23 mmol of chlorobenzene by mmol of Pd. After the 1st use the catalyst was removed magnetically and a new load of chlorobenzene and solvent was added to the reactor. Similar TON of ca. 22 mol_{CB}/mol_{Pd} with experimental error of ±5 was observed indicating a good recovery and reutilization of the catalyst.

This process opens the possibility to obtain these carbon coated magnetic particles from any iron containing material, including different synthetic iron oxides (Fe_2O_3, Fe_3O_4, FeOOH, etc.), naturally occurring iron oxides or even iron containing wastes (e.g., red mud, and mining waste).

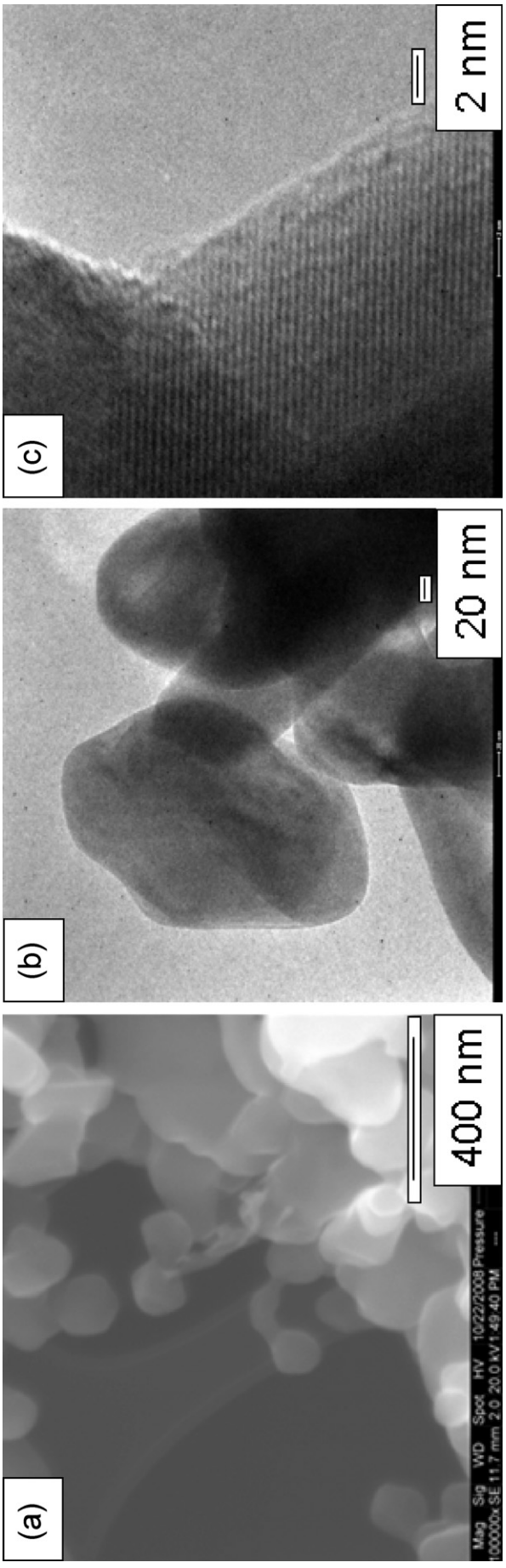

Fig. 10. (a) SEM and (b and c) HRTEM images of the suspended particles of the sample HtM700.

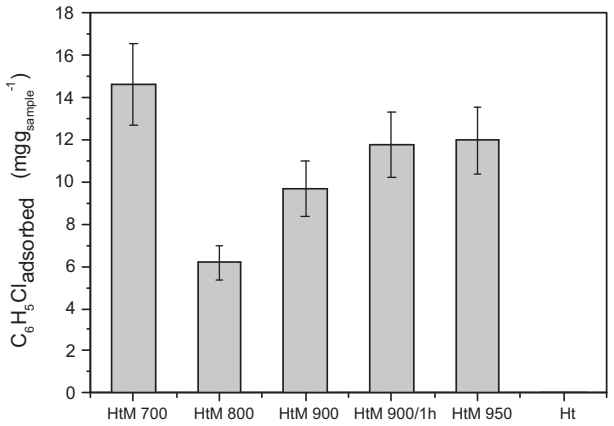

Fig. 11. Chlorobenzene adsorption (ChlB) by hematite and the materials produced after reaction of hematite and methane at different temperatures and times.

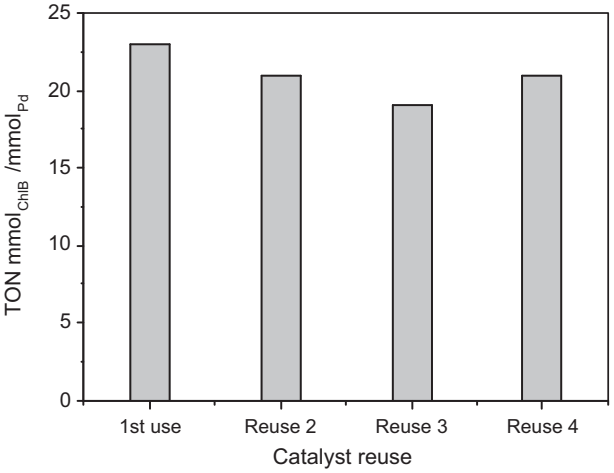

Fig. 12. Chlorobenzene to benzene conversion (turn over number-TON) by the Pd(5%)/HtM700 catalyst.

4. Conclusions

The combined reduction/CVD process using methane and hematite is a versatile, technically simple and low cost method to produce carbon coated Fe_3O_4 particles. TEM images, elemental analyses, TG, chlorobenzene adsorption, Raman, TPR and the resistance to acid attack strongly suggest the formation of a very thin carbon coating on the Fe_3O_4 nanoparticles surface. The obtained material can be separated into two fractions by simple dispersion in water, i.e., a settled material composed of micrometric magnetic particles and the suspended material composed of nanoparticles with average size of 100–200 nm. The magnetic particles were investigated in a preliminary work as adsorbent for model contaminant organic molecules in water and also to produce a magnetic recyclable supported Pd catalyst used for the hydrogen-dechlorination reaction showing promising results. This process opens the possibility to obtain these magnetic particles from any iron containing material, including different synthetic iron oxides (Fe_2O_3, Fe_3O_4, FeOOH, etc.), naturally occurring iron oxides or even iron containing wastes (e.g., red mud, mining waste).

Acknowledgements

The authors acknowledge the support of FAPEMIG, PRPq/UFMG, CNPq, FINEP and CAPES. Thanks for the images provided by the UFMG microscopy center.

Appendix A. Supplementary data

Supplementary data associated with this article can be found, in the online version, at doi:10.1016/j.materresbull.2011.01.008.

References

[1] L.C.R. Machado, F.W.J. Lima, R. Paniago, J.D. Ardisson, K. Sapag, R.M. Lago, Appl. Clay Sci. 31 (2006) 207.
[2] L.C.A. Oliveira, R.V.R.A. Rios, J.D. Fabris, R.M. Lago, K. Sapag, J. Chem. Educ. 81 (2004) 248.
[3] L.C.A. Oliveira, R.V.R.A. Rios, J.D. Fabris, K. Sapag, V.K. Garg, R.M. Lago, Appl. Clay Sci. 22 (2003) 169.
[4] L.C.A. Oliveira, R.V.R.A. Rios, J.D. Fabris, V.K. Garg, K. Sapag, R.M. Lago, Carbon 40 (2002) 2177.
[5] D.E. Sosnovik, M. Nahrendorf, R. Weissleder, Basic Res. Cardiol. 103 (2008) 122.
[6] D.L.J. Thorek, A. Chen, J. Czupryna, A. Tsourkas, Ann. Biomed. Eng. 34 (2006) 23.
[7] Z.Y. Ma, H.Z. Liu, Chin. Particuol. 5 (2007) 1.
[8] B. Shen, Y. Li, Z.F. Wang, N.Y. He, Chin. J. Catal. 28 (2007) 509.
[9] M.J. Jacinto, P.K. Kiyohara, S.H. Masunaga, R.F. Jardim, L.M. Rossi, Appl. Catal. A 338 (2008) 52.
[10] X.L. Zhao, Y.L. Shi, T. Wang, Y.Q. Cai, G.B. Jiang, J. Chromatogr. A 1188 (2008) 140.
[11] S. Veintemillas-Verdaguer, Y. Leconte, R. Costo, O. Bomati-Miguel, B. Bouchet-Fabre, M.P. Morales, P. Bonville, S. Pérez-Rial, I. Rodriguez, N. Herlin-Boime, J. Magn. Magn. Mater. 311 (2007) 120.
[12] G.M. Shi, Z.D. Zhang, H.C. Yang, J. Alloys Compd. 384 (2004) 296.
[13] Z.F. Wang, P.F. Mao, N.Y. He, Carbon 44 (2006) 3277.
[14] P.Y. Keng, I. Shim, B.D. Korth, J.F. Douglas, J. Pyun, ACS Nano 1 (2007) 279.
[15] E.N. Konyushenko, N.E. Kazantseva, J. Stejskal, M. Trchová, J. Kovářová, I. Sapurina, M.M. Tomishko, O.V. Demicheva, J. Prokeš, J. Magn. Magn. Mater. 320 (2008) 231.
[16] S. Gyergyek, M. Huskić, D. Makovec, M. Drofenik, Colloids Surf. A: Physicochem. Eng. Aspects 317 (2008) 49.
[17] M.K. Hong, B.J. Park, H.J. Choi, Phys. Status Solidi A: Appl. Mater. Sci. 204 (2007) 4182.
[18] J.S. Qiu, Y.F. Li, Y.P. Wang, Y.L. An, Z.B. Zhao, Y. Zhou, W. Li, Fuel Process Technol. 86 (2004) 267.
[19] R. Fernandez-Pacheco, M. Arruebo, C. Marquina, R. Ibarra, J. Arbiol, J. Santamaria, Nanotechnology 17 (2006) 1188.
[20] D.Y. Geng, Z.D. Zhang, W.S. Zhang, P.Z. Si, X.G. Zhao, W. Liu, K.Y. Hu, Z.X. Jin, X.P. Song, Scripta Mater. 48 (2003) 593.
[21] R. Sergiienko, E. Shibata, Z. Akase, H. Suwa, T. Nakamura, D. Shindo, Mater. Chem. Phys. 98 (2006) 34.
[22] L.S. Panchakarla, A. Govindaraj, Bull. Mater. Sci. 30 (2007) 23.
[23] W.Z. Wu, Z.P. Zhu, Z.Y. Liu, Y.I. Xie, J. Zhang, T.D. Hu, Carbon 41 (2003) 317.
[24] H.M. Cao, G.J. Huang, S.F. Xuan, Q.F. Wu, F. Gu, C.Z. Li, J. Alloys Compd. 448 (2008) 272.
[25] D.C. Wei, Y.Q. Liu, L.C. Cao, L. Fu, X.L. Li, Y. Wang, G. Yu, J. Am. Chem. Soc. 129 (2007) 7364.
[26] P. Singjai, K. Wongwigkarn, Y. Laosiritaworn, R. Yimnirun, S. Maensiri, Curr. Appl. Phys. 7 (2007) 662.
[27] J.S. Qiu, Q.X. Li, Z.Y. Wang, Y.F. Sun, H.Z. Zhang, Carbon 44 (2006) 2565.
[28] Z.B. Zhang, H.F. Duan, S.H. Li, Y.J. Lin, Langmuir 26 (2010) 6676.
[29] Z. Wang, H. Guo, Y. Yu, N. He, J. Magn. Magn. Mater. 302 (2006) 397.
[30] J. Zhang, J. Du, Y. Qian, Q. Yin, D. Zhang, Mater. Sci. Eng. B 170 (2010) 51.
[31] W.M. Zhang, X.L. Wu, J.S. Hu, Y.G. Guo, L.J. Wan, Adv. Funct. Mater. 18 (2008) 3941.
[32] H. Liu, G. Wang, J. Wang, D. Wexler, Electrochem. Commun. 10 (2008) 1879.
[33] S.H. Xuan, L.Y. Hao, W.Q. Jian, X.L. Gong, Y. Hu, Z.Y. Chen, Nanotechnology 18 (2007) 35602.
[34] J. Lee, Y. Lee, J.K. Youn, H. Bin Na, T. Yu, H. Kim, S.M. Lee, Y.M. Koo, J.H. Kwak, H.G. Park, H.N. Chang, M. Hwang, J.G. Park, J. Kim, T. Hyeon, Small 4 (2008) 143.
[35] J.C. Tristão, F.C.C. Moura, R.M. Lago, K. Sapag, Quím. Nova 33 (2010) 1379.